# Europium Doped Magnesium Zinc Sulfophosphate Glass as Potential Red Laser Host

**I M Danmallam[a,c], H Bhaktiar[a,b], R Ariffin[a], I Bulus[a,d], S K Ghoshal[*a,b]**
[a]Phosphor Research Group & AOMRG, Department of Physics, Faculty of Science, Universiti Teknologi Malaysia, 81310 Skudai, Johor, Malaysia.
[b]Laser Centre and Advance Optical Materials Research Group, , Department of Physics, Faculty of Science, Universiti Teknologi Malaysia, 81310 Skudai, Johor, Malaysia.
[c]Sokoto Energy Research Center, Usmanu Danfodiyo University Sokoto, Sokoto, Nigeria.
[d] Department of Physics, School of Sciences, Kaduna State College of Education Gidan waya, Kafanchan, Nigeria.

Email: sibkrishna@utm.my, ibrahimdanmallam @gmail.com

**Abstract.** Demand for rare earth ions (REIs) doped inorganic glasses have been ever-increasing for diverse photonic applications. Synthesis of these glasses needs the appropriate choice of suitable host matrices, modifiers, and REIs as dopants to improve their spectroscopic traits. In this realization, a new series of magnesium-zinc-sulfophosphate glasses were prepared with varied europium ions ($Eu^{3+}$) doping contents (0 to 2.0 mol%). Such melt-quench synthesized glasses were characterized at room temperature by diverse analytical techniques to determine their physical and optical properties. XRD pattern of as-quenched samples confirmed their amorphous nature. Densities of the glass system were observed to increase from 2.540 to 2.788 $g.cm^{-3}$ with the increase in $Eu^{3+}$ doping contents from 0 to 2.0 mol% which were attributed to the generation of more bridging oxygen atoms and enhanced network compactness. Photoluminescence (PL) emission spectra of glasses exhibited four characteristic peaks positioned at 593, 613, 654 and 701 nm assigned to corresponding $^5D_0 \rightarrow {}^7F_0$, $^5D_0 \rightarrow {}^7F_2$, $^5D_0 \rightarrow {}^7F_3$, and $^5D_0 \rightarrow {}^7F_4$ transitions in $Eu^{3+}$, in which the intensity of the peak at 613 nm (red) was highest. Emission intensities of all peaks were enhanced with the rise in $Eu^{3+}$ content up to 1.5 mol% and quenched thereafter. It was affirmed that the physical and optical traits of these glass compositions can be improved by adjusting the $Eu^{3+}$ doping contents. The proposed glass compositions may be potential for the development of varied photonic devices especially for eye safe solid-state red laser and fibre sensors.

## 1. Introduction

It has been established that the high solubility of rare earth ions (REIs) in the oxide glass host matrix is beneficial for the improvement various properties of the host materials. Despite such exceptional physiochemical properties of oxide glass hosts the low quantum efficiency, the concentration dependent emission intensity quenching and small absorption coefficient of REIs doped glasses limits their practical applications [1]. Trivalent europium ion ($Eu^{3+}$) display $^5D_0 \rightarrow {}^7F_2$ transition (deep in red colour at 613 nm) in the presence of non-degenerate $^7F_0$ (ground) and $^5D_0$ (excited) states [2]. Repeated researches revealed that incorporation of metallic nanostructures (with varied morphologies and concentrations) into the glass system can significantly modify their structure and physical properties, thereby influence the PL emission intensity of the phosphor. Energy efficiency, environmental friendliness (devoid of mercury pollution), higher illumination, ease of installation and

conveyance over incandescent fluorescent bulbs truly make glass based phosphors gifted materials [3]. For most of the REIs doped oxide glasses the spectroscopic properties are intensively studied to see their feasibility for practical device applications. In this regard, the Judd-Ofelt (J-O) intensity parameters ($\Omega_2$, $\Omega_4$ and $\Omega_6$) and radiative properties as well as the nephelauxetic ratio and the bonding parameters were routinely calculated to support the measured spectroscopic and structural characteristics.

Considering the abovementioned significant attributes of REIs doped phosphate-based glasses, in this work we synthesized and characterized a series of (65–$x$) $P_2O_5$–20MgO-15$ZnSO_4$–$xEu_2O_3$ glasses (where $x$ was varied from 0.0 to 2.0 mol%) using melt-quenching method. As-synthesized glasses were characterized using various analytical techniques to assess their physical and structural properties. PL spectra were used to determine the emission cross-section. Besides, J-O intensity and radiative parameters were calculated to complement the experimental spectroscopic data. The achieved results were analysed, interpreted, discussed and compared. The proposed glass compositions with improved optical traits were shown to be effective for the development of various efficient photonic devices.

## 2. Experimental procedures

High purity phosphorus pentoxide, magnesium oxide, zinc sulfate, europium oxide and silver chloride (purchased from Sigma Aldrich) were used as raw chemicals for the glass preparation. The melt quenching method was used for the glass synthesis. Depending on the nominal glass composition, these chemicals (without further purification) were weighed and placed in an alumina crucible before being melted in an electrical furnace at 1100 ºC for 90 minutes. Upon achieving the required viscosity, the melt was dispensed onto metal plate and annealed at 300 °C for 180 minutes before being cooled down to room temperature. The molar composition of glasses molar composition (65−$x$) $P_2O_5$–20MgO–15$ZnSO_4$–$xEu_2O_3$ ($x$ = 0.0, 0.5, 1.0, 1.5 and 2.0) were prepared using melt-quenching method. As-quenched samples were coded as MZSPE0.0, MZSPE0.5, MZSPE1.0, MZSPE1.5 and MZSPE2.0 depending on $Eu_2O_3$ contents. Synthesized glasses were cut and polished to achieve desired transparency and uniform thickness for further characterizations.

The amorphous character of the as-quenched samples was confirmed using X-ray diffraction analyses (Rigaku X-ray Diffractometer that used Cu-Kα radiations of wavelength, $\lambda \simeq 1.54$ Å) operated at 40 kV and 40 mA, scanning angle (2θ) range of 10-80º, step size of 0.02º and resolution of 0.01º. Jeol JSMeIT300LV (operated at 30 kV with 10 mm resolution) was used to record elemental maps and EDX spectra. Absorption spectra of studied glasses in the range of 350–2500 nm (at resolution of ±1 nm) were recorded by Shimadzu UVPC-3101 spectrophotometer.

## 3.0 Result and Discussions

### *3.1 Structural properties*

Figure 1 shows the XRD pattern of two selected as-quenched samples (MZSPE0.5 and MZSPE2.0). Complete absence of any characteristic structural long-range order clearly confirmed their amorphous nature. It did not show any crystallization peak and revealed a broad hump at 25° which is the character of glassy or amorphous system [4].

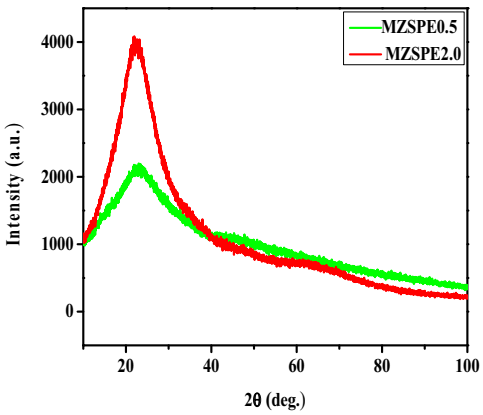


**Figure 1.** XRD pattern of MZSPE0.5 and MZSPE2.0 glasses.

Figure 2 and 3 depicts EDX spectra and EDX maps of the glasses ascertaining the presence of right elements (Eu, Zn, Mg, O, S and P in Wt%) in the glass system and their regular homogenous distribution within the disorder network, respectively. Appearance of sharp peak at 1.5 keV indicated the existence of oxygen in the sample. The EDX maps of MZSPE2.0 glass depicted homogeneous distribution of elements within glass system [5].

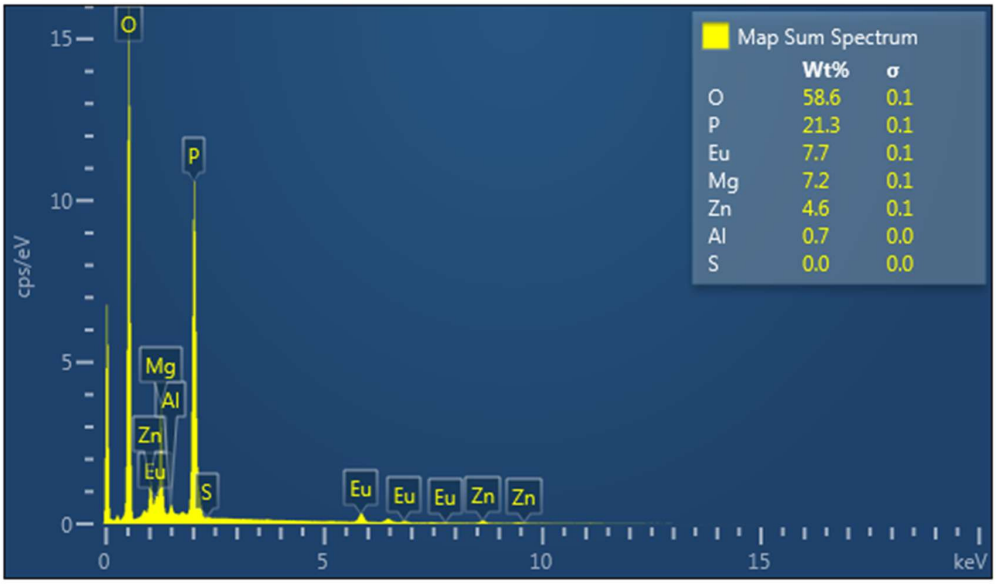


**Figure 2.** EDX pattern of MZSPE2.0 glass.

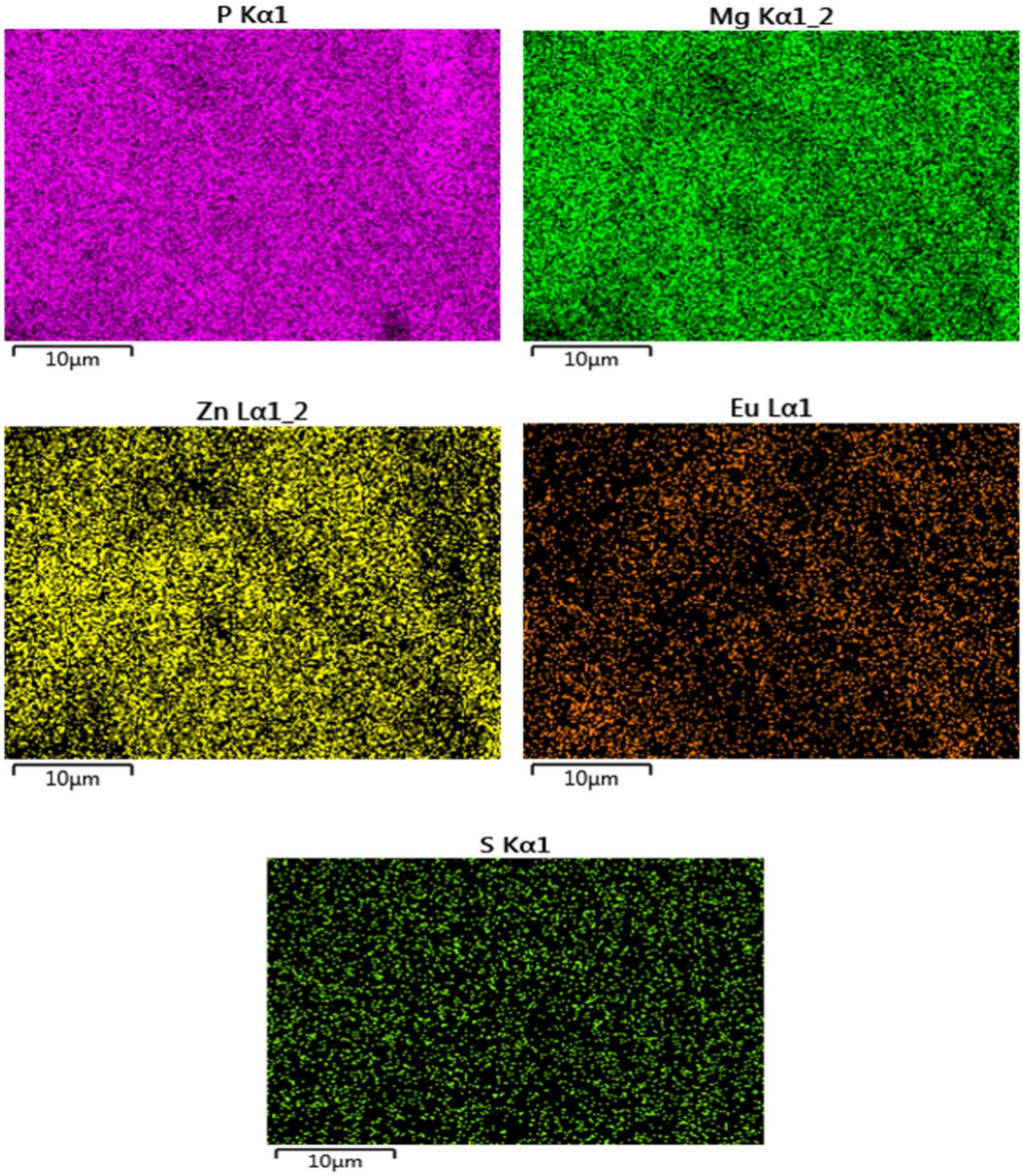


**Figure 3.** Elemental composition mapping in the MZSPE2.0 glass.

*3.2 Optical properties*

Figure 4 (a) and (b) shows the absorption spectra of synthesized glasses in visible and NIR region, respectively. The former one (Figure 4 (a)) consisted of six peaks and the later (Figure 4 (b)) composed of two peaks which aroused from the ground state to excitation state transitions of $Eu^{3+}$. Six visible absorption peaks centred at 360, 380, 394, 414, 465, and 531 nm corresponded to $^7F_0 \rightarrow {}^5L_6$, $^7F_0 \rightarrow {}^5G_4$, $^7F_1 \rightarrow {}^5L_6$, $^7F_1 \rightarrow {}^5D_3$, $^7F_0 \rightarrow {}^5D_2$ and $^7F_1 \rightarrow {}^5D_1$ transitions in $Eu^{3+}$. Besides the appearance of two NIR peaks at 2091 and 2205 nm were allotted to $^7F_6 \rightarrow {}^7F_0$ and $^7F_1 \rightarrow {}^7F_6$ transitions in $Eu^{3+}$ [6] . Irrespective of $Eu^{3+}$ concentration variation, the peak positions of all spectral transition remained unchanged which was attributed to the weak crystal field interaction in the proposed glass system [7]. The occurrence of inhomogeneous broadening in the absorption peak affirmed the disorder nature of the glass network.

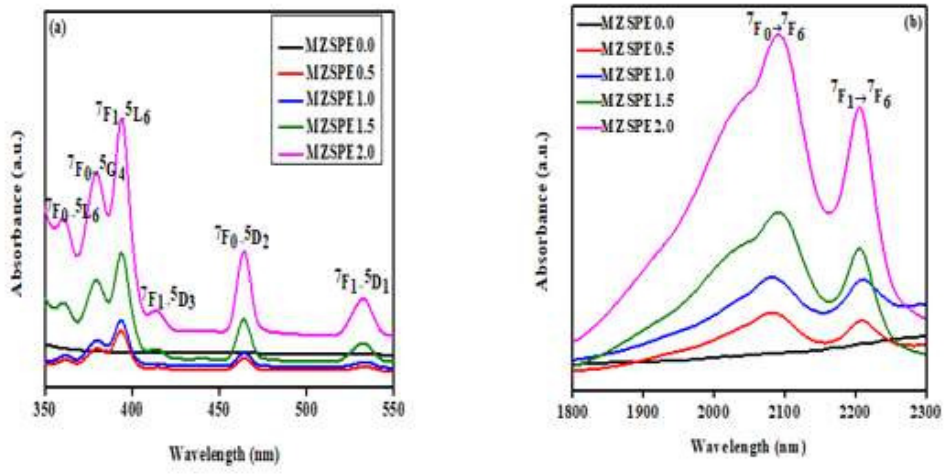


**Figure 4.** Absorption spectra of the glasses in the (a) visible region and (b) NIR region.

Table 1 presents the observed band position ($cm^{-1}$), their assignments and the bonding parameters (β and δ) of studied glasses. By exploring the $Eu^{3+}$ ligand bond, the nephelauxetic ratio in terms of ligand field properties and the bonding parameter yields.

$$\sigma = \left( \frac{1-\bar{\beta}}{\bar{\beta}} \right) \times 100 \tag{1}$$

with

$$\bar{\beta} = \frac{v_c}{v_a} \tag{2}$$

where $v_c$ and $v_a$ denotes the respective energies (in $cm^{-1}$) of glass host for equivalent transition in aquo and complex ions.

The $Eu^{3+}$ contents dependent variation in the average nephelauxetic ratios and bonding parameters of glasses. Ionic or covalent character among ligand and metal ion were verified using the bonding parameter (δ) demonstrating improve covalency of the synthesized glasses with values range from (-0.000371 to 0.00726) as shown in table 1.

**Table 1.** Band locations ($cm^{-1}$), assignments and bonding parameters (β and δ) of synthesized glasses.

| Transitions | MZSPE0.5 | MZSPE1.0 | MZSPE1.5 | MZSPE2.0 | Aquo |
|---|---|---|---|---|---|
| $^7F_0 \rightarrow {}^5L_6$ | 27777.8 | 27777.8 | 27472.5 | 27624.3 | 27670 |
| $^7F_0 \rightarrow {}^5G_4$ | 26315.9 | 26525.2 | 26246.7 | 26109.7 | 26620 |
| $^7F_0 \rightarrow {}^5L_6$ | 25380.7 | 25445.3 | 25316.5 | 25000 | 25400 |
| $^7F_1 \rightarrow {}^5D_3$ | 24154.6 | 24178.6 | 24200.4 | 24120.7 | 24038 |
| $^7F_0 \rightarrow {}^5D_2$ | 21505.4 | 21551.7 | 21598.3 | 21505.4 | 21519 |
| $^7F_1 \rightarrow {}^5D_1$ | 18832.4 | 18761.7 | 18726.6 | 18761.7 | 19028 |
| $^7F_0 \rightarrow {}^7F_6$ | 17006.8 | 16666.7 | 16611.2 | 16583.5 | 16638.9 |
| β | 1.000371 | 0.999957 | 0.995390 | 0.99274 | 1 |
| δ | -0.00371 | 0.000043 | 0.00461 | 0.00726 | 0 |

Figure 5 displays the excitation spectra of a selected glass obtained at 613 nm. It consisted of eight excitation peaks positioned at 364, 376, 381, 433, 463, 533, 593 and 613 nm assigned to the transitions of $^7F_0 \rightarrow {}^5L_{10}$, $^7F_0 \rightarrow {}^5L_8$, $^7F_0 \rightarrow {}^5L_7$ at 381, $^7F_0 \rightarrow {}^5L_6$, $^7F_0 \rightarrow {}^5D_2$, $^7F_1 \rightarrow {}^5D_1$, $^7F_1 \rightarrow {}^5D_0$ and $^5D_0 \rightarrow {}^7F_2$. The peak appeared at 613 nm was more pronounced and hence selected for recording emission spectra of prepared glasses ranged from of 550–720 nm [8].

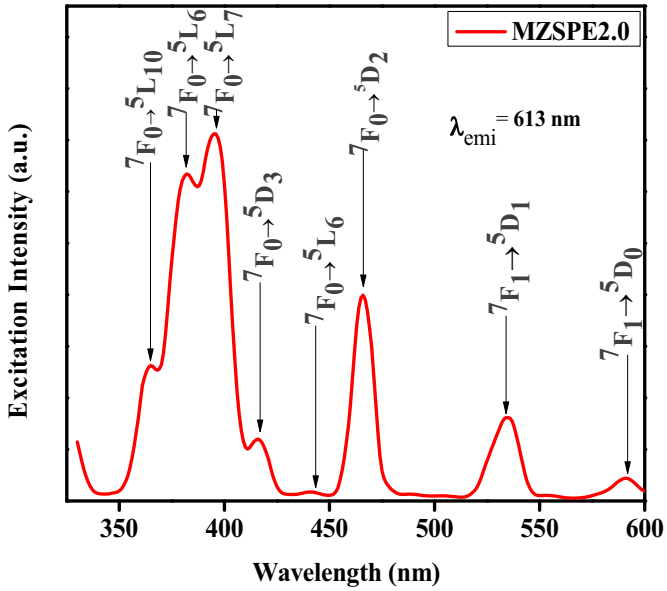


**Figure 5** :Excitation spectra of MZSPE2.0.

*3.3 Photoluminescence spectra*

Figure 6 depicts the PL emission spectra of studied glasses which exhibited four significant peaks centred at 593, 613, 654, and 701 nm. The most intense PL peak appeared at 613 nm (red) clearly showed the potential of the proposed glass system towards solid state laser development provided the stimulated emission cross-section of this transition is high [9]. To verify this argument, the oscillator strength, J-O intensity and radiative parameter, stimulated emission cross-section and quality factor of this emission transition was further calculated. Additionally, the band at 593 nm was allotted to the magnetic dipole (MD) transition ($^5D_0 \rightarrow {}^7F_1$) and the one at 613 nm was endorsed to the electric dipole (ED) transition ($^5D_0 \rightarrow {}^7F_2$) of $Eu^{3+}$ [10]. The revelation of these two emission spectral transition in $Eu^{3+}$ was attributed to their separation into low phonon energy [11].

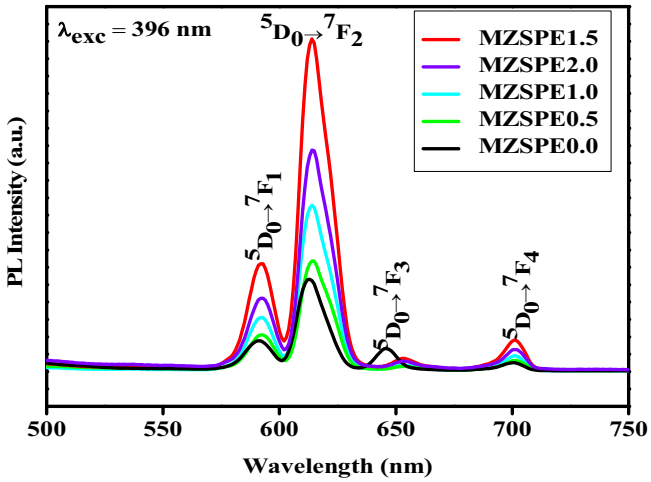


**Figure 6.** Room temperature PL emission spectra of synthesized glasses.

*3.4 Judd-Ofelt intensity and radiative parameters*

This theory provides a way of ascertaining the spectral line of transition, fundamentally Judd-Ofelt theory govern a set of parameters (t = 2, 4, 6), using absorption or emission spectra, in a least of square fit difference. The limited transitions of $^7F_0$ and $^7F_1$ ground state to various excited state such as $^5D_1$, $^5D_2$ and $^5L_6$ of the transitions of europium ion in absorption spectra necessitated the use of emission spectra for Judd-Ofelt analysis. The most important factor in J-O parameters is stimulated emission cross section as a significant lasing material[13]. The higher simulated emission cross section makes the material good potential for solid state laser application [14]. Intensity parameter $\Omega_2$ are linked to ligand field asymmetry around rare earth ion while $\Omega_4$ are connected to rigidity and bulk properties of ions medium. The nonexistence of $^5D_0 \rightarrow {}^7F_6$ transition disallowed omega 6 ( $\Omega_6$) to be found as such it is taken as zero [15]. The intensity ratio (R) value of $^5D_0 \rightarrow {}^7F_2$ and $^5D_0 \rightarrow {}^7F_1$ decrease with proportional europium ions concentration increase signifying high asymmetry and covalent bond atmosphere among REI and ligands of oxygen.

$$\frac{\int I_J d\nu}{\int I_1 d\nu} = \frac{A_J}{A_1} = \frac{e^2 \nu_J^3}{S_{md} \nu_1^3} \times \frac{n\left(n^2+2\right)^2}{9n^3} \Omega_t \left\| U^t \right\|^2 \quad (3)$$

where parameters $\Omega_t$ are evaluated from the intensity ratios of transitions and vj wavenumber of transitions

$$\frac{n\left(n^2+2\right)^2}{9n^3} \quad (4)$$

where n is refractive index.

The intensity ratio is often used in determining the host material quality providing symmetry information around $Eu^{3+}$ covalency, higher R (R > 1) signifies lower symmetry while (0 < R < 1) characterize higher symmetry. Table 3 shows the R rate of MZSPE glasses where R values decrease and then subsequently increase from 4.012 to 2.96 but the R value of 4.012 shows high laser potential of the glass material [16]. Table 2 compares linear trend of Judd Ofelt parameter values with that of existing literature where The MZSPE0.5 glass exhibited highest value of $\Omega_2$. The $\Omega_2$ values decline from 14.4 $\times 10^{-20}$ $cm^2$ to 10.7$\times 10^{-20}$ $cm^2$ with RE increase from 0.5 mol% to 2.0 mol% largely attributed to generation of bridging oxygen. The reduced $\Omega_2$ values increases the ionicity of the glass

system thus having more network symmetric structure in relation to others reported but MZSPE2.0 increases showing high covalency totally incoherent with nephelauxetic ratio.

**Table 2.** The Judd-Ofelt intensity parameters comparison with different glasses.

| Glass code | $\Omega_2$ | $\Omega_4$ | Trend | Ref. |
|---|---|---|---|---|
| MZSPEu0.0 | 14.4 | 1.26 | $\Omega_2 > \Omega_4$ | Present work |
| MZSPEu1.0 | 10.7 | 2.52 | $\Omega_2 > \Omega_4$ | Present work |
| MZSPEu1.5 | 11.3 | 2.23 | $\Omega_2 > \Omega_4$ | Present work |
| MZSPEu1.75 | 11.2 | 1.83 | $\Omega_2 > \Omega_4$ | Present work |
| MZSPEu2.0 | 12.6 | 2.10 | $\Omega_2 > \Omega_4$ | Present work |
| Lithium fluoroborate | 6.60 | 3.50 | $\Omega_2 > \Omega_4$ | [17] |
| Oxyfluoroborate | 3.45 | 2.93 | $\Omega_2 > \Omega_4$ | [18] |
| telluroborate | 5.54 | 1.09 | $\Omega_2 > \Omega_4$ | [19] |
| Silicate | 4.23 | 1.04 | $\Omega_2 > \Omega_4$ | [20] |
| phosphate | 11.9 | 3.8 | $\Omega_2 > \Omega_4$ | [21] |
| Germanate | 4.81 | 1.41 | $\Omega_2 > \Omega_4$ | [47] |

**Table 3**. Compared transition ratio intensity (R) of $^5D_0 \rightarrow {}^7F_2$ to $^5D_0 \rightarrow {}^7F_1$ of MZSPE glasses.

| Glass composition | $R=\frac{^5D_0 \rightarrow {}^7F_2}{^5D_0 \rightarrow {}^7F_1}$ | Ref. |
|---|---|---|
| MZSPE0.5 | 4.01 | Present work |
| MZSPE1.0 | 2.98 | Present work |
| MZSPE1.5 | 2.96 | Present work |
| MZSPE2.0 | 3.15 | Present work |
| PKSAEU10 | 4.43 | [15] |
| PAZE20 | 2.55 | [16] |
| KBZFB | 2.7 | [22] |
| EFBA | 0.7 | [23] |
| $KLA(PO_3)_4$ | 1.659 | [24] |

Table 4 depicts results of transition probabilities ($A_{rad}$), branching ratios (Br), stimulated emission cross section of excited state, optical band width and optical gain width of $^5D_0 \rightarrow {}^7F_2$ for $Eu^{3+}$ in various concentrations. The important parameter for laser design that characterize prospect of achieving stimulated emission in all the transitions[25]The above 0.5 value of branching ratio symbolises potential laser transition within the glass medium, cross section informs a possible laser potential which shows energy excitation rate from the lasing material estimated from emission spectrum [26]. Intensity parameters follow trend which indicates structural changes in europium (III) ion surrounding (short range effects) and covalent nature dominancy, whereas $\Omega_4$ is correlated to bulk properties like inflexibility and viscosity[27]. Superior intensity of parameter $\Omega_2$ suggest hypersensitive transition $^5D_0 \rightarrow {}^7F_2$ transition indicating $Eu^{3+}$ ions are situated around extremely polarizable chemical environment around the REIs [28]. High numerical value of $\Omega_2$ signifies great symmetry and covalency character of $Eu^{3+}$ ions ligand bond which shows improved homogeneity of converse parity electronic composition liable for spectral intensity discrepancy [29].

$$A_{ed} = \left( \frac{64\pi^4 \nu^3}{3h(2J+1)} \right) \left( \frac{n(n^2+2)^2}{9} \right) S_{ed} \tag{5}$$

From equation 5, where $(A_{ed})$ represent electric dipole and $(A_{md})$ represent magnetic dipole transition probabilities

$$\beta_r = \frac{A_{rad}}{\sum A_{rad}} \tag{6}$$

$\beta_r$ is the fluorescence branching being the ratio of radiative transition probability to total radiative transition probability to all levels.

$$\tau_{cal} = \frac{1}{\sum A_{rad}} \tag{7}$$

the calculated radiative lifetime, $\tau_{cal}$ of an emitting state is related to its total radiative transition probability to all sublevels

**Table 4.** Fluorescence branching ratio ($\beta_{r,}$), Radiative transition probability ($A_{rad}$,$s^{-1}$), emission band position ($\lambda_p$,nm), total radiative transition probability ($A_{T,}s^{-1}$), calculated lifetime ($\tau_{cal}$,ms), emission cross section ($\sigma\times10^{-22}$ $cm^2$) emission cross section ($\sigma\times10^{-22}$ $cm^2$), gain bandwidth ($\sigma\times FWHM\times10^{-20}$ $cm^2$) and optical gain ($\sigma\times\tau_{cal}\times10^{-25}$ $cm^2$ $s^{-1}$) for (65 − x)$P_2O_5$ 20MgO 15$ZnSO_4$–x $Eu_2O_3$

| Transition | Parameter | MZSPEu0.5 | MZSPEu1.0 | MZSPEu1.5 | MZSPEu2.0 |
|---|---|---|---|---|---|
| $^5D_0 \rightarrow {}^7F_1$ | $\lambda_p$ | 591 | 591 | 591 | 591 |
| | $A_{rad}$ | 181.76 | 181.634 | 179.994 | 178.30 |
| | $\beta_r$ | 0.196 | 0.235 | 0.228 | 0.212 |
| | $\sigma$ | 4.78 | 4.765 | 3.81 | 3.78 |
| | $\sigma\times FWHM$ | 0.613 | 0.613 | 0.607 | 0.602 |
| | $\sigma\times\tau_{cal}$ | 5.154 | 6.16 | 4.84 | 4.49 |
| $^5D_0 \rightarrow {}^7F_2$ | $\lambda_p$ | 615 | 615 | 615 | 615 |
| | $A_{rad}$ | 715.74 | 531.417 | 437.66 | 612.709 |
| | $\beta_r$ | 0.771 | 0.687 | 0.687 | 0.729 |
| | $\sigma$ | 18.64 | 13.860 | 0.15 | 16.9 |
| | $\sigma\times FWHM$ | 2.815 | 2.09 | 2.18 | 2.41 |
| | $\sigma\times\tau_{cal}$ | 20.09 | 17.9 | 19.1 | 20.2 |
| $^5D_0 \rightarrow {}^7F_4$ | $\lambda_p$ | 701 | 701 | 701 | 701 |
| | $A_{rad}$ | 30.39 | 60.74 | 373.47 | 49.562 |
| | $\beta_r$ | 0.033 | 0.079 | 0.079 | 0.59 |
| | $\sigma$ | 2.04 | 40.2 | 3.25 | 3.03 |
| | $\sigma\times FWHM$ | 0.202 | 0.404 | 0.354 | 0.33 |
| | $\sigma\times\tau_{cal}$ | 2.20 | 5.20 | 4.25 | 3.6 |
| | $A_T$ ($s^{-1}$) | 927.89 | 773.795 | 788.629 | 840.57 |
| | $\tau_{cal}$ (ms) | 1.077 | 1.292 | 1.268 | 1.189 |

## 4.0 Conclusion

For the first-time optical properties of $Eu^{3+}$ doped magnesium-zinc-sulfophosphate glasses were experimentally measured and then analysed using J-O theory. Photoluminescence emission spectra were used to evaluate the J-O intensity and radiative parameters. The ligand interaction in the glasses exhibited strong ionic character regardless of $Eu^{3+}$ contents from (-0.000371 to 0.00726). REIs clustering induced PL intensity quenching was evidenced in MZSPE2.0. Excellent radiative properties such as branching ratio in the range of 0.687 to 0.771 and emission cross section ranging from ($0.15\times10^{-22}$ $cm^2$ – $40.2\times10^{-22}$ $cm^2$) shown by the proposed glasses confirmed their effectiveness as laser active medium. Coherent trends in the J-O intensity parameters ($\Omega_2>\Omega_4$) indicate its potential for laser applications.

**Acknowledgements**
The authors would like to express their appreciation to the sponsors with UTM KTP NMG project No 4Y161, Tier 1-18H78, FRGS-5F050 and Sokoto Energy Research Centre, Usmanu Danfodiyo University Sokoto, Nigeria

## References

[1] Komaraiah D, Radha E, James J, Kalarikkal N, Sivakumar J, Ramana Reddy MV, Sayanna R 2019 *J. Lumin.* **211** 320–333
[2] Danmallam IM, Krishna S, Ariffin R, Aisha S 2018 *Malaysian J. Fundam. Appl. Sci*. **222** 78–82
[3] Chen L, Deng X, Zhao E, Chen X, Xue S, Zhang W, Chen S, Zhao Z, Zhang W, Chan TS 2014 *J. Alloys Compd*. **613** 312–316
[4] Shajan D, Murugasen P, Sagadevan S 2017 *Optik (Stuttg)*. **136** 165–171
[5] Segawa H, Cho Y, Sekiguchi T, Hirosaki, Deguchi K, Ohki S, Shimizu T 2018 *J. Eur. Ceram. Soc.* **38** 735–741
[6] Sudheendra HS, Darshan GP, Basavaraj RB, Naik YV, Premakumar HB, Nagabhushana H, Williams JF, Hareesh K, Kokila MK 2019 *Opt. Mater. (Amst)*. **90** 159–171
[7] Xinqiang Yuan XY, Long Zhang LZ, Jin He JH, Yan Wang YW, Rihong Li, RL 2014 *Chinese Opt. Lett.* **12** 071602–071604
[8] Vijaya N, Jayasankar CK 2013 *J. Mol. Struct.* **1036** 42–50
[9] Righini GC, Ferrari M 2005 *Riv. Del Nuovo Cim.* **28** 1–53
[10] Khaidir REM, Fen YW, Zaid MHM, Matori KA, Omar NAS, Anuar MF, Wahab SAA, Azman AZK 2019 *Optik (Stuttg).* **182** 486–495
[11] Han J, Talbot J, McKittrick J 2010 *Chinese Opt. Lett*. **15** 183–190
[12] Xia H, Zhang J, Wang J, Zhang Y, Haiping Xia, Jianli Zhang et al., *Chin. Opt. Lett.* **4** 476-479
[13] Mohd Saidi MSA, Ghoshal SK, Arifin R,Roslan MK, Muhammad R, Shamsuri WNW, Abdullah M, Shaharin MS 2018 *J. Alloys Compd*. **754** 171–183
[15] Linganna K, Jayasankar CK 2012 *Spectrochim. Acta - Part A Mol. Biomol. Spectrosc.* **97** 788–797
[16] Saad M, Stambouli W, Mohamed SA, Elhouichet H, 2012 *J. Alloys Compd*. **705** 550–558
[17] Gupta SK, Mohapatra M, Kaity S, Natarajan V, Godbole SV 2012 *J. Lumin*. **132** 1329–1338
[18] Annapoorani K, Marimuthu K 2017 *J. Non. Cryst. Solids.* **463** 148–157
[19] Pravinraj S, Vijayakumar M, Marimuthu K 2017, *Phys. B Phys. Condens. Matter*. **509** 84–93
[20] Moustafa SY, Sahar MR, Ghoshal SK 2017 *J. Alloys Compd.* **712** 781–794
[21] Ahmadi F, Hussin R, Ghoshal SK 2016 *J. Non. Cryst. Solids.* **452** 266–272
[22] Gopi S, Jose SK, George A, Unnikrishnan NV, Joseph C, Biju PR 2018 *J. Mater. Sci. Mater. Electron.* **29** 674–682
[23] Devi R, Dalal M, Bala M, SP Khatkar, Taxak VB, Boora P 2016 *J. Mater. Sci. Mater. Electron.* **27** 12506–12516
[24] Ferhi M, Bouzidi C, Horchani-Naifer K, Elhouichet H, Ferid 2015 *J. Lumin.* **157** 21–27
[25] Danmallam IM, Ghoshal SK, Ariffin R, Jupri SA, Sharma S 2019 *J. Lumin*. 216
[26] Ram GC, Narendrudu T, Suresh S, Kumar AS, Rao MVS, Kumar VR, Rao DK 2017 *Opt. Mater.*

*(Amst)*. **66** 189–196
[27] Bulus I, Hussin R, Ghoshal SK, Tamuri AR, Jupri SA 2019 *Ceram. Int.* 0–1.
[28] Ćirić A, Stojadinović S, Dramićanin MD, *Opt. Mater. (Amst)*. **88** 392–395
[29] Danmallam IM, Ghoshal SK, Ariffin R, Jupri SA, Sharma S, Bulus I 2019 *Optik (Stuttg)*. **196** 163197